Journal of Power Sources 295 (2015) 259–267

Contents lists available at ScienceDirect

Journal of Power Sources

journal homepage: www.elsevier.com/locate/jpowsour

Cross-linked anion exchange membranes with pendent quaternary pyrrolidonium salts for alkaline polymer electrolyte membrane fuel cells

Chunhua Lan, Jun Fang*, Yingjie Guan, Huili Zhou, Jinbao Zhao

Department of Chemical & Biochemical Engineering, College of Chemistry and Chemical Engineering, Xiamen University, Xiamen 361005, PR China

HIGHLIGHTS

- Novel anion exchange membranes based on pyrrolidonium salts and PVA were prepared.
- The properties of the membranes could be tuned by varying the blending ratios.
- The membranes showed excellent thermal, chemical and dimensional stability.
- The membranes displayed the high OH^- conductivity of above 10^{-2} S cm^{-1} at 25 °C.
- A peek power density of 88.9 mW cm^{-2} of the H_2/air fuel cell was obtained at 65 °C.

ARTICLE INFO

Article history:
Received 1 April 2015
Received in revised form
4 June 2015
Accepted 6 July 2015
Available online 15 July 2015

Keywords:
Anion exchange membrane
Fuel cell
Pyrrolidonium
Cross-linking
Polymerization

ABSTRACT

Novel anion-exchange membranes based on two kinds of pyrrolidonium type ionic liquids, N-methyl-N-vinyl-pyrrolidonium (NVMP) and N-ethyl-N-vinyl-pyrrolidonium (NVEP), have been synthesized via polymerization and crosslinking treatment, followed by membrane casting. The covalent cross-linked structures of these membranes are confirmed by FT-IR. The obtained membranes are also characterized in terms of water uptake, ion exchange capacity (IEC), ionic conductivity as well as thermal, dimensional and chemical stability. The membranes display hydroxide conductivity of above 10^{-2} S cm^{-1} at 25 °C. Excellent thermal stability with onset degradation temperature above 235 °C, good alkaline stability in 6 mol L^{-1} NaOH at 60 °C for 168 h and remarkable dimensional stability of the resulting membranes have been proved. H_2/air single fuel cells employed membrane M3 and N3 show the open-circuit voltage (OCV) of 0.953 V and 0.933 V, and the maximum power density of 88.90 mW cm^{-2} and 81.90 mW cm^{-2} at the current density of 175 mA cm^{-2} and 200 mA cm^{-2} at 65 °C, respectively.

1. Introduction

With the energy crisis and the environment pollution becoming serious, polymer electrolyte membrane fuel cells have received increasing attentions and have been regarded as the ideal alternative of fossil fuel. In particular, proton exchange membrane fuel cells (PEMFC) have been identified as the most promising power sources for vehicular transportation, power generation and portable power supply [1–4]. However, there are still many obstacles impeding the commercial utilizations of PEMFCs, such as slow electrode-kinetics, CO poisoning of expensive Pt-based electrode catalysts, high fuel permeability and complex water management [3,5–7].

Alkaline anion exchange membranes fuel cells (AAEMFCs), which use the alkaline anion exchange membranes (AEMs) to displace the proton-exchange membranes (PEMs) with OH^- anions instead of H^+ cations [8], could address the issues of the shortcomings of PEMFCs. In alkaline condition, the fuel cell efficiency can be increased and non-noble metal catalysts can be used [9–11].

As the core component of AAEMFC, the properties of AEM directly affect the performance of the cell. The traditional preparation methods of AEM mainly include the chloromethylation and quaternization of the pristine polymers, such as poly (ether ether ketone) (PEEK) [12,13], polysulfone [14], poly (phthalazinon ether

* Corresponding author.
E-mail addresses: 651300819@qq.com (C. Lan), jfang@xmu.edu.cn (J. Fang), ihuagong@163.com (Y. Guan), zhouhuili9988@qq.com (H. Zhou), jbzhao@xmu.edu.cn (J. Zhao).

http://dx.doi.org/10.1016/j.jpowsour.2015.07.015
0378-7753/

sulfone ketone) (PPESK) [15], and radiation-grafted PPO [16] and FEP [9]. Another approach is directly polymerization of monomers containing chloromethyl groups or quaternary ammonium groups [17–19]. However, the AEMs functionalized with alkyl quaternary ammonium groups are proved to be unstable due to nucleophilic substitution and (or) Hofmann elimination reaction, especially at high pH and elevated temperature [20]. In a series of previous studies, we have reported the preparation and characterization of AEMs based on imidazolium type ionic liquids (IILs) [21–23] since 2010. Although these membranes exhibit the promising performances in application of AAEMFC, the previous studies encountered the following problems: the high price and toxicity of the imidazolium type ionic liquids. Aiming to exploit cost-effective AEMs with good thermal and chemical stability, suitable ionic conductivity, and sufficient mechanical strength, the cross-linked AEMs based on pyrrolidonium type IILs and poly (vinyl alcohol) (PVA) were studied in this work. We believe that the quaternary pyrrolidonium salt groups are stable than the conventional quaternary alkyl ammonium salt groups at high pH and elevated temperature due to resonance effect of the pyrrolidonium cation. The raw materials, both PVA and N-vinyl-pyrrolidone (NVP) are low-cost and environmentally friendly materials with good performances, such as film-forming capacities, hydrophilic properties and chemical stability [24–27]. Due to the nucleophilicity and steric accessibility of N atom in the NVP, the quaternarization could be carried out [28].

The dimensional stability is another problem associated with AEMs. Both PVA and poly (pyrrolidonium salt) are strong hydrophilic materials, so cross-linking process were adopted to suppress the membrane swelling. As an alternative way, a lot of membranes prepared by semi-interpenetrating polymer network (SIPN) show good performances due to the polyelectrolyte immobilized into a polymer cross-linked network matrix [29,30].

To our knowledge, the AEM functionalized with quaternary pyrrolidonium salt for alkaline fuel cell application has not been reported before. In this work, we originally report the preparation and characterization of two kinds of cross-linked AEMs functionalized with pendent quaternary pyrrolidonium salts. Fourier transform infrared spectroscopy (FT-IR), nuclear magnetic resonance (NMR) and elemental analysis are used for characterization of ionic monomer, while FT-IR is employed for structural characterization of their membranes. The hydroxide conductivity, water uptake (WU), IEC, thermal stability, and alkaline stability of the membranes are measured to evaluate their applicability in alkaline fuel cells. In addition, the membrane electrode assembly (MEA) based on the resulting AEMs were used for preliminary H_2/air fuel cell test.

2. Experiment

2.1. Material

NVP (99%, containing 100 ppm sodium hydroxide as inhibitor) and bromoethane (BrE, 98%) were purchased from Aladdin Industrial Corporation, PVA (99% hydrolyzed, average molecular weight: Mw = 86,000–89,000) was purchase from Sigma–Aldrich Corp., glutaraldehyde (GA, 25 wt% aqueous solution), 2, 2′-azobisiso butyronitrile (AIBN) and iodomethane (IM, Chemical pure) were purchased from China National Medicines Corporation Ltd. NVP was purified by distillation before used.

2.2. Synthesis of anion exchange resins

To obtain anion exchange resins, poly (N-methyl-N-vinyl-pyrrolidonium) (PNVMP) and poly (N-ethyl-N-vinyl-pyrrolidonium) (PNVEP), the following two synthesis routes and preparation process were studied in this work.

(i) NVP was quaternized with halohydrocarbon, followed by polymerization.

Firstly, a mixture of NVP and halohydrocarbon was added in a three-neck round-bottomed flask and magnetic stirred under nitrogen atmosphere to synthesize quaternary pyrrolidonium salt, NVMP or NVEP. After the reaction completed, the viscous product was extracted by cyclohexane for three times to remove the unreacted reactants, then dried in a vacuum oven for 12 h at 25 °C. Secondly, the product was dissolved in deionized (D.I) water and then ammonium persulfate and sodium bisulfate were added into the solution under nitrogen atmosphere successively. Ionic polymerization was performed at 65 °C for 12 h. The resulting halogenated polymers, named as PNVMP-1 and PNVEP-1, were purified by washing with cyclohexane and then dried in vacuum oven at 50 °C for 24 h Scheme 1 demonstrates the synthesis route of PNVMP-1 and PNVEP-1.

(ii) NVP was homopolymerized, quaternization followed.

Firstly, radical polymerization of NVP was carried out using AIBN as an initiator and ethanol as a solvent at 65 °C for 12 h under nitrogen protection. After polymerization, the product was extracted by cyclohexane for three times and then dried in a vacuum oven for 12 h at 25 °C. The dried product was added into a three-neck round-bottomed flask with absolute ethanol and then quaternized with halohydrocarbon. The resulting polymers were extracted by cyclohexane and then dried in vacuum oven at 50 °C for 24 h. The polymers were labeled as PNVMP-2 and PNVEP-2 and Scheme 2 describes the synthesis route of them.

2.3. Preparation of alkaline membranes

Solution-casting method was employed to prepare membranes in this work. Firstly, appropriate amounts of the obtained polymers were added to the PVA solution, which was prepared by dissolving PVA in distilled water and then heating at 80 °C with continuous stirring to form a 10 wt% transparent solution. The blending of PVA and the anion exchange resin (AER) in different mass ratios were investigated. Then, a specified volume of crosslinking agent (5 wt% GA aqueous solution) was added to the blending solution. After that, the homogeneous and transparent solutions were cast onto glass pane and then dried in a vacuum oven at 60 °C for 8 h. The membrane with a thickness of about 40–70 μm was peeled from the glass pane and put into electrically heated drying cabinet at 130 °C for 1 h and then soaked in a crosslinking agent (10 wt% GA acetone solution) for about 1 h. The cross-linked membranes were soaked in 1 mol L^{-1} NaOH solution at room temperature for 48 h to

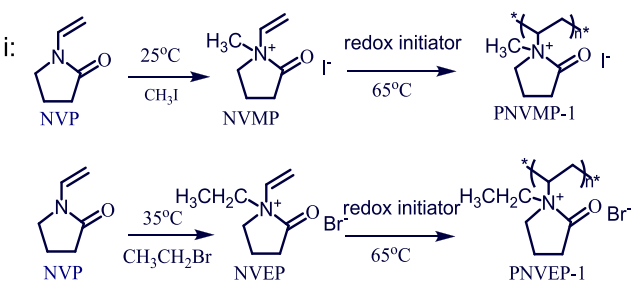

Scheme 1. Synthetic route of PNVMP-1 and PNVEP-1.

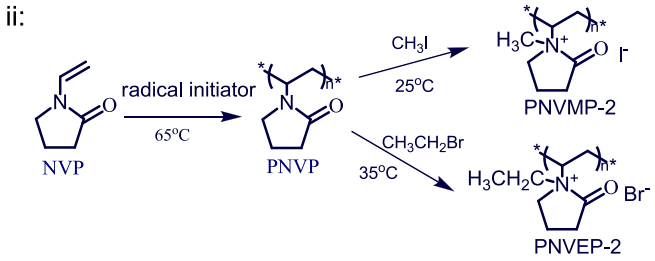

Scheme 2. Synthetic route of PNVMP-2 and PNVEP-2.

exchange the Br^- (or I^-) to OH^-. The resulting OH^- form membranes were named as [PNVMP/PVA]OH and [PNVEP/PVA]OH, respectively. Finally, the membranes were thoroughly washed with D.I water until the solutions were neutral and then stored in D.I water for further use. The process diagram of the preparation of X^-(Br^- or I^-) form membranes was given in Scheme 3.

2.4. Morphological and structure characterization

The molecular weight of polymers was tested by Gel Permeation Chromatography (GPC) (Waters 2695, America). The FT-IR spectra were scanned using an infrared spectrometer (VERTEX 70, Germany) with a wavenumber resolution of 0.4 cm^{-1} in the range from 4000 to 600 cm^{-1}. The ^1H NMR spectra of the ionic monomer were recorded on a 500 MHz NMR spectrometer (Bruker Ascend III, Germany). The N contents were measured by an Elemental Analyzer (Vario EL III, Germany). The thermal stability of membranes was performed by Thermo Gravimetric Analyzer (TG 209, Netzsch), where the samples of 5 mg loaded into an alumina oxide pan were heated from 30 to 600 °C at a heating rate of 10 °C min^{-1} under a nitrogen atmosphere. The tensile strength of the membrane was tested by Universal material testing machine (SUN 2500, Italy).

2.5. Water uptake (WU)

Water uptake of the OH^- form membranes was determined by evaluating the mass change before and after immersing in deionized water [31]. The membranes were dried at 60 °C under vacuum until constant dried weights were obtained. Then the dry membranes were immersed in deionized water at room temperature

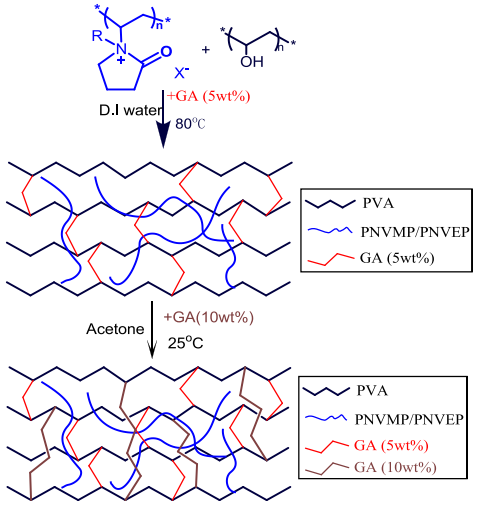

Scheme 3. The preparation of X^-(Br^- or I^-) form membranes.

and periodically weighed until constant water uptake weights were recorded. The water uptake was calculated by the follow:

$$WU\ (\%) = \frac{W_{wet} - W_{dry}}{W_{dry}} \times 100\% \quad (1)$$

where W_{wet} and W_{dry} are the weights of the fully hydrated membrane and of dry membrane, respectively.

The swelling degree (%) was measured by a linear expansion ratio, evaluated by the difference between wet and dry dimensions of membrane sample. The swelling degree was calculated by the equation:

$$\text{Swelling degree}(\%) = \frac{L_{wet} - L_{dry}}{L_{dry}} \times 100\% \quad (2)$$

where L_{wet} and L_{dry} are the length of the wet and the dry membranes, respectively [19].

2.6. Ion exchange capacity (IEC)

IEC of the membrane was measured by back-titration method. A certain weight of dry OH^- form membranes were immersed into 0.1 mol L^{-1} HCl solution at room temperature for about 48 h to completely exchange the OH^- to Cl^-. Then the solutions were titrated with standard 0.1 mol L^{-1} NaOH solutions. The IEC of the anion exchange membrane was calculated from the hydrochloric acid amount and the weight of the dry membrane as following:

$$IEC\left(\text{mmol g}^{-1}\right) = \frac{M_{1,HCl} - M_{2,HCl}}{W_{dry}} \quad (3)$$

where $M_{1,HCl}$ and $M_{2,HCl}$ are moles of HCl before and after equilibrium, respectively, and W_{dry} is the weight of the dry membrane.

2.7. Ionic conductivity

The conductivities of the OH^- form membranes were measured by two-probe AC impedance technique with Parstat 263 electrochemical equipment (Princeton Advanced Technology, USA). Membrane samples were clamped between two stainless steel electrodes and the resistance through the plane was measured, as described in our previous works [15,17,21,22,32]. Impedance spectra were recorded in the frequency ranging from 1 to 10^6 Hz and all the membranes were equilibrated in deionized water. A Bode plot was plotted to check the frequency region where the impedance had a constant value, and the resistance was obtained from the associated Nyquist plot. During the test, the membrane samples should avoid to exposure in air. Ionic conductivity was calculated as following:

$$\sigma\left(\text{S cm}^{-1}\right) = \frac{L}{R \times A} \quad (4)$$

where L (cm) is the distance between two stainless steel electrodes, R(Ω) is the resistance of the membrane, and A(cm^2) is the surface area of the membrane exposed to the electric field.

2.8. MEA fabrication and fuel cell test

The MEA consisted of an AEM, catalyst layers (40 wt% Pt, Johnson Matthey), and diffusion layers (Teflon-treated carbon paper, Toray-250). The preparation process included the following three steps. Firstly, catalyst inks were prepared by mixing catalyst with 5 wt% OH^- form membranes in DMF solution and propylene

glycol. The ink was sonicated for 15 min, and then magnetic stirred for 24 h at room temperature to get a homogeneous solution. Then the catalyst ink was sprayed onto the carbon paper to deposit a catalyst layer with the expected load of Pt. The active electrode area for a single cell test was 4 cm^2. The OH^- form AEM was sandwiched with the electrodes and then hot-pressed at 0.8 MPa for 10 min at 45 °C. The MEA was assembled into a single fuel cell with serpentine flow channels. H_2 at the anode and air at the cathode were fed with the given flow rate. Single cell test was performed using an electronic load (ZY8714, ZHONGYING Electronic Co., Ltd., China).

3. Results and discussions

3.1. The effect of quaternarization time and agents

The synthesis routes of NVMP and NVEP are shown in Scheme 1 and Scheme 2. To preliminary confirm whether the quaternarization had occurred, determinands, CH_3I, CH_3CH_2Br, NVP, as well as NVMP and NVEP, were added into 5 wt‰ silver nitrate solutions, respectively. The experimental phenomena are listed in Table 1. It can be seen that precipitate come out of the solution when the determinand is NVMP (or NVEP). However, there is no obvious change can be observed for CH_3I, CH_3CH_2Br, or NVP used as the determinand. The results indicate that the halide ions are created in NVMP and NVEP.

The preparation process of anion exchange membrane involves quaternization, polymerization, crosslinking and alkalization. Among them, quaternization is a key reaction that determines the ionic conductivity of the membrane. Therefore, it is highly important to study the effect factors on quaternization. To evaluate influence of quaternization time on the anion exchange resin, nitrogen contents of PNVMP and PNVEP were investigated by elemental analysis. Nitrogen only exist in the pyrrolidonium groups, hence, the quaternization degrees of the polymers can be calculated from nitrogen content by comparing the experimental values and the theoretical nitrogen values. From the results showed in Table 2 and Table 3, it can be seen that the N content decreased gradually whereas the degree of quaternization increase with the increasing of quaternization time for the same polymer that prepared by the same route. Both of them tend to be stable after 48 h, thereafter, only a small increase of quaternization degree can be obtained when we continue to increase the quaternization time.

From the Tables 2 and 3, it is observed that the degree of quaternization of the PNVMP is higher than that of the PNVEP under the same synthetic route and quaternization time. This is due to methyl iodide has the smaller molecular volume compared with bromoethane, which leads to the smaller steric hindrance when attacks the nitrogen atom of pyrrolidone ring. It is also observed that the degrees of the quaternization of the same polymers prepared by route (i) are higher than that of the polymers prepared by route (ii) under the same quaternization time, which can be explained by that the lower steric hindrance of the NVP monomer compared with its self-polymerization product when quaternization reaction is carried out. In addition, the molecular weight of PNVMP-1d, PNVMP-2d, and PNVEP-1d, and PNVEP-2d were measured by GPC instrument. As shown in Table 4, the molecular weights of all samples are in the same order of magnitude. The above results indicate that the synthetic route (i) is a better way to synthesize target polymers compared with route (ii), and the optimized quaternization time is 48 h.

According to the previous experimental results and analysis results, the polymers, PNVMP-1d and PNVEP-1d, were selected to further studies.

3.2. Solubility of the polymers

The solubility of the polymer is an important parameter for forming membrane. The solubility of the polymer is investigated by dissolving a certain amount of polymer in different solvents at room temperature and the results are summarized in Table 5. It can be seen that both PNVMP-1d and PNVEP-1d are soluble in some polar, protic solvents such as water, ethanol, isopropanol, and also soluble in some polar, aprotic solvents, such as DMF and acetone. They are insoluble in nonpolar solvents such cyclohexane, diethyl ether and ethyl acetate, even at elevated temperature. Because the polymers can be dissolved in water due to the strongly hydrophilic groups of quaternary pyrrolidonium salt, they can be cast into films, but cannot be directly used in fuel cells before a crosslinking process. Crosslinking process is a common method to suppress membrane solubility and swelling in water. The crosslinking of the membrane will be discussed in detail in subsequent section.

3.3. Chemical structure analysis

3.3.1. FT-IR spectra analysis

Fig. 1 shows the FT-IR spectra analysis of NVP, NVMP, NVEP, PNVMP-1d and PNVEP-1d. Compared with the spectra of NVP, a new absorption peak at 3425 cm^{-1} appearing in spectra of NVMP, NVEP, PNVMP-1d and PNVEP-1d is assigned to the stretch vibration of −OH, which illustrates the products possess strong water imbibition after quaternization. The peaks between 2800 and 3000 cm^{-1} are the characteristics of alkyl, and these peaks are found to be substantially enhanced after quaternization, which is likely attributed to the vibration of the methyl or ethyl introduced from halohydrocarbon.

The sharp peak at 1704 cm^{-1} in NVMP and NVEP is identified to the asymmetric stretching of C═O bond of the pyrrolidone ring, which is migrated to 1658 cm^{-1} in spectra of PNVMP-1d and PNVEP-1d. The peak at 1628 cm^{-1} appearing in spectra of NVMP and NVEP belongs to the stretch vibration of C═C from the side chain of pyrrolidone and it disappears in spectra of PNVMP-1d and PNVEP-1d, which might be due to the polymerization of NVMP and NVEP.

3.3.2. NMR analysis

The obtained NVMP and NVEP were characterized by 500 MHz ^1H NMR in $CDCl_3$ and the resulting ^1H NMR data of NVMP was as following. ^1H NMR ($CDCl_3$, δ ppm relative to TMS): δ = 7.12–7.07 (dd, H), δ = 4.47–4.45 (d, H), δ = 4.40–4.37 (d, H), δ = 3.54–3.51 (t, 2H), δ = 2.51–2.48 (t, 2H), δ = 2.16 (s, 3H), δ = 2.15–2.08 (m, 2H). The ^1H NMR data of NVEP was as following. ^1H NMR ($CDCl_3$, δ ppm relative to TMS): δ = 7.12–7.07 (dd, H), δ = 4.45–4.43 (d, H),

Table 1
The halide ion detection by the silver nitrate solution.

	Determinand				
	CH_3I	CH_3CH_2Br	NVP	NVMP	NVEP
The experiment phenomena	–	–	–	yellow precipitation	faint yellow precipitate

(–) no obvious change.

Table 2
The experimental N content[a] and the degree of quaternization of the polymers synthesized by route i.

Polymer	Quaternization time(h)	N content (wt %)	Degree of quaternization (%)
PNVMP-1a	12	8.69	35.28
PNVMP-1b	24	7.87	47.12
PNVMP-1c	36	7.42	54.72
PNVMP-1d	48	6.99	62.91
PNVMP-1e	72	6.86	65.58
PNVEP-1a	12	9.65	31.24
PNVEP-1b	24	8.79	44.27
PNVEP-1c	36	8.23	54.23
PNVEP-1d	48	7.98	59.12
PNVEP-1e	72	7.88	61.16

[a] The theoretical N content of PNVMP and PNVEP are 5.53 wt% and 6.36 wt% respectively.

Table 3
The experimental N content[a] and the degree of quaternization of the polymers synthesized by route ii.

Polymer	Quaternization time(h)	N content (wt %)	Degree of quaternization (%)
PNVMP-2a	12	9.19	29.10
PNVMP-2b	24	8.73	34.76
PNVMP-2c	36	7.97	45.54
PNVMP-2d	48	7.55	52.43
PNVMP-2e	72	7.38	55.44
PNVEP-2a	12	10.59	19.41
PNVEP-2b	24	9.82	28.93
PNVEP-2c	36	9.42	34.49
PNVEP-2d	48	9.12	38.98
PNVEP-2e	72	9.07	39.76

[a] The theoretical N content of PNVMP and PNVEP are 5.53 wt% and 6.36 wt% respectively.

Table 4
Molecular weight of the polymers.

Sample	Molecular weight		
	M_n	M_w	M_w/M_n
PNVMP-1d	38294	61023	1.594
PNVMP-2d	59842	77019	1.287
PNVEP-1d	44183	69455	1.572
PNVEP-2d	61018	88462	1.450

M_n: number-average molecular weight; M_w: weight-average molecular weight.

$\delta = 4.40–4.37$ (d, H), $\delta = 3.54–3.51$ (t, 2H), $\delta = 3.45–3.41$ (q, 2H), $\delta = 2.51–2.48$ (t, 2H), $\delta = 2.15–2.08$ (m, 2H), $\delta = 1.69–1.66$ (t, 3H).

The results of FT-IR spectra analysis and ^{1}H NMR analysis indicated the successful preparation of the ionic monomers, NVMP and NVEP.

3.4. Effect of the blending ratio on the performance of membranes

In order to explore the best blending ratio, the WU, ionic conductivity and IEC of membranes were measured. The OH^- form membrane samples with different blending ratios studied in this paper were listed in Table 6 and the results were displayed in Fig. 2 and Fig. 3. It can be seen that the relationship between blending ratio and WU, ionic conductivity or IEC has similar trends. As the content of PVA in the blending solution increases, WU, ionic conductivity or IEC gradually increases, reaches the maximum, and then decreases. After the crosslinking treatment, the membranes become completely insoluble in water by introducing the special cross-linkable groups into the polymer structure. The introduction of PVA is very helpful to retain the dimensional stability of the membrane; however, excess PVA leads to decline of ion conductivity of the membrane, because the PVA is free from anion exchange functional groups. By tuning the blending ratio, an appropriate WU and a relatively high ionic conductivity can be achieved. For example, the WU, IEC, ionic conductivity of cross-linking membrane sample M3 is 66.2%, 1.607 mmol g^{-1}, 2.05×10^{-2} S cm^{-1}, respectively. For membrane sample N3, the WU, IEC, ionic conductivity is 63.4%, 1.052 mmol g^{-1} and 1.57×10^{-2} S cm^{-1}, respectively.

3.5. FT-IR spectra of the cross-linked membrane

The FT-IR spectra of the cross-linked membrane M3 and N3 are shown in Fig. 4. The new peak at 1130 cm^{-1} appeared in these two spectra is corresponding to the vibration of C–O–C [33], which indicates the presence of covalent cross-linked structure after cross-linking treatment. The peak of 1288 cm^{-1} appeared in both Figs. 1 and 6 is the characteristic peak of C–N of pyrrolidone ring, which indicates that the structure of pyrrolidone in the PNVMP or PNVEP is not destroyed by the cross-linking reaction.

Table 5
The dissolution performance of polymers.

Polymer	Solvent							
	Water	Ethanol	DMF	Isopropanol	Acetone	Cyclohexane	Diethyl ether	Ethyl acetate
PNVMP-1d	+	+	+	+	+	×	×	×
PNVEP-1d	+	+	+	+	+	×	×	×

(+)Soluble at the room temperature; (×) Insoluble.

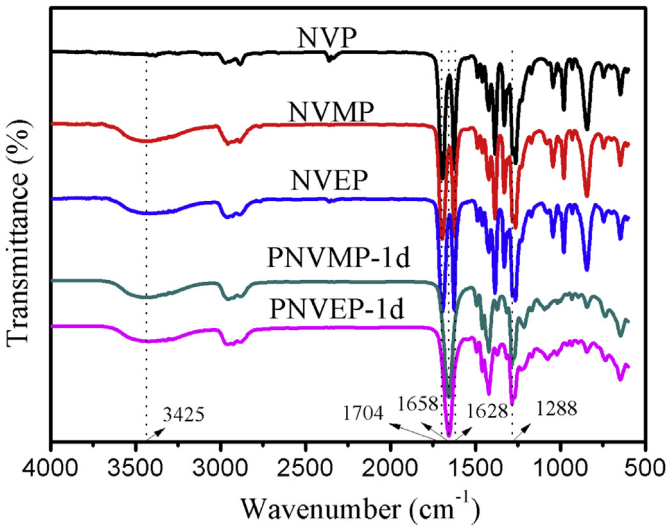

Fig. 1. FTIR spectra of NVMP, NVEP, PNVMP-1d and PNVEP-1d.

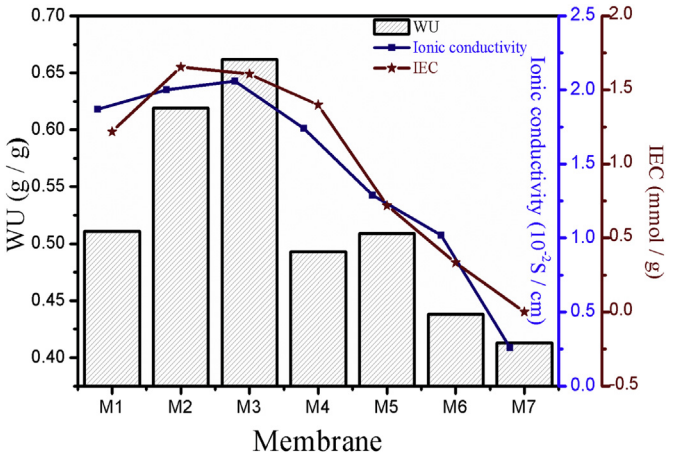

Fig. 2. The effect of blend ratio on the WU, IEC and ionic conductivity of membrane [PNVMP/PVA]OH.

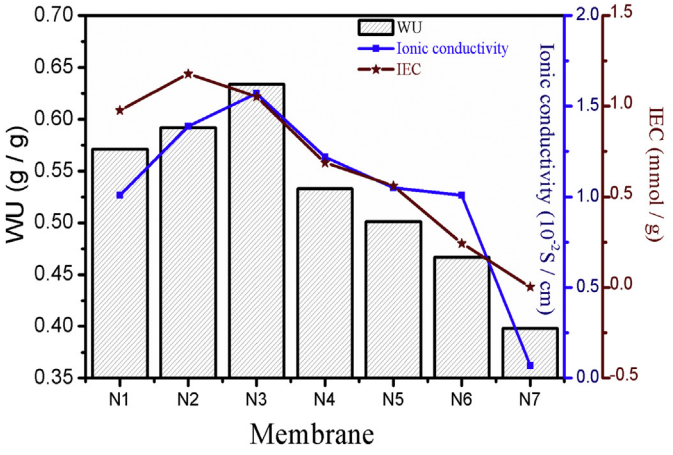

Fig. 3. The effect of blend ratio on the WU, IEC and ionic conductivity of membrane [PNVEP/PVA]OH.

3.6. The effect of temperature on the ionic conductivity

It has been reported that operation of AEMFCs at elevated temperature lead to enhanced performances [32]. High temperature would not only reduce thermodynamic voltage losses due to potential pH gradients through the membrane but also improve electro kinetics [34]. The influence of temperature on ionic conductivity of OH^- form membrane is studied. As the temperature rises from 25 °C to 85 °C, ionic conductivity of membrane M3 increases from 2.05×10^{-2} S cm^{-1} to 4.98×10^{-2} S cm^{-1}, while ionic conductivity of membrane N3 increases from 1.57×10^{-2} S cm^{-1} to 4.14×10^{-2} S cm^{-1}. The results shows that the ionic conductivities of membrane M3 and N3 gradually increase with the increasing temperature, which can be explained by faster migration of ions and higher diffusivity with the increasing of temperature [33]. The membrane M3 exhibits higher ionic conductivity than membrane N3 at the same temperature, which is due to the higher quaternization degree of membrane M3.

The Ln σ vs. 1000/T plot is shown in Fig. 5. Assuming that the conductivity follows the Arrhenius behavior, the apparent activation energy (E_a) of the cross-linked membrane can be obtained according to the Arrhenius equation:

$$E_a = -b \times R \quad (5)$$

where b is the slope of the line regression of ln σ(S cm^{-1}) vs. 1000/T (K^{-1}) plots, and R is the gas constant (8.314 J K^{-1} mol^{-1}). The apparent activation energies of membrane M3 and N3 are calculated to be 13.83 kJ mol^{-1} and 14.05 kJ mol^{-1}, respectively.

3.7. Thermal and chemical stability

3.7.1. Thermal stability

The thermal stability of the membrane is one of the key metrics for AEM applied to fuel cell [35,36]. The measurements were carried out on PVA, PNVMP, PNVEP and membrane M3 and N3, and the results were shown in Fig. 6. Results show that both membrane M3 and N3 display three weight lose stages around 30–130, 235–370, and 370–450 °C. The first weight loss stage (about 5%) the loss of residual water in the samples. As shown in the TG curves, the second weight loss (about 60%) between 235 and 370 °C are corresponding to the decomposition of PVA [37]. The third weight loss (about 35%) of membrane M3 and N3, beginning at about 370 °C, are considered to be caused by the degradation of main chain of the PNVMP and PNVEP [38]. These TG curves reveal that both membrane M3 and N3 have good thermal stabilities and high degradation temperatures.

3.7.2. Chemical stability

Due to the AEMFCs work under high pH condition and elevated

Table 6
The designation of membrane by the blend ratio of Polymer/PVA.

Membrane	Blend ratio/g g^{-1}						
	0.35/0.35	0.30/0.40	0.25/0.45	0.20/0.50	0.15/0.55	0.10/0.60	0.0/0.70
[PNVMP/PVA]OH	M1	M2	M3	M4	M5	M6	M7
[PNVEP/PVA]OH	N1	N2	N3	N4	N5	N6	N7

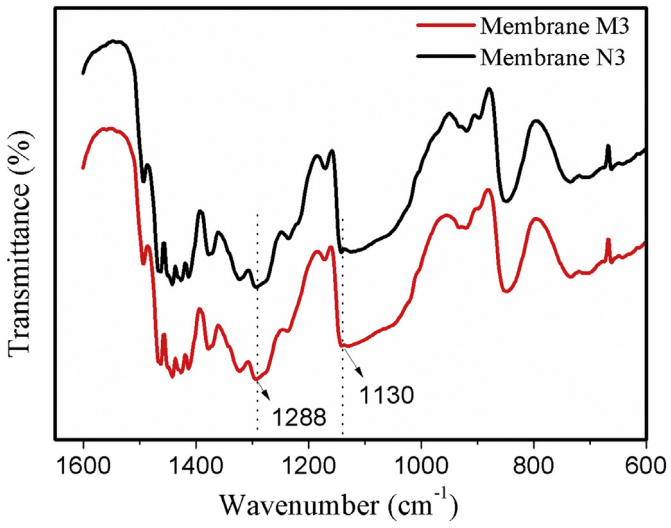

Fig. 4. FT-IR spectra of membrane M3 and N3.

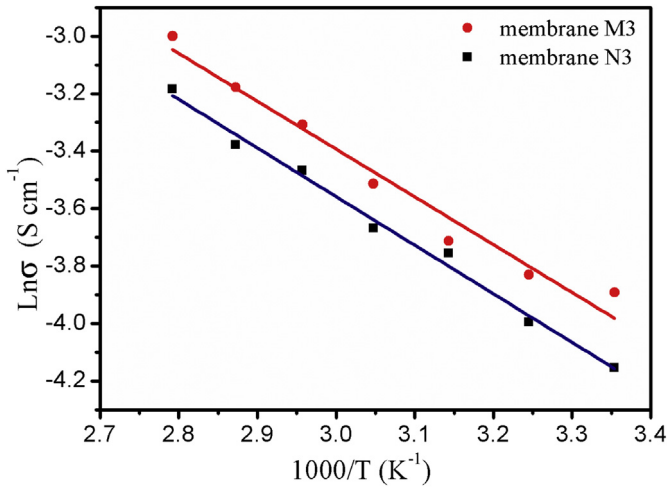

Fig. 5. Temperature dependence of ionic conductivity by plotting Ln σ vs. 1000/T.

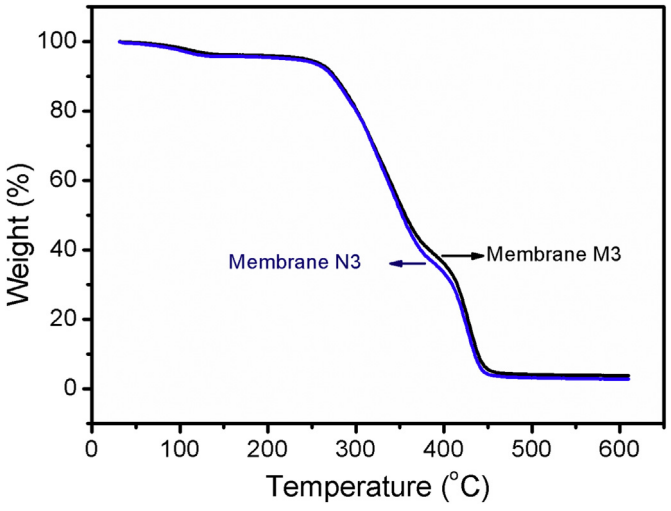

Fig. 6. Thermo Gravimetric analysis of membrane M3 and N3.

temperature, and AEMs with quaternary ammonium functional groups decompose readily by either an E2 (Hofmann degradation) mechanism or an SN2 substitution reaction [20,39]. So, it is important to develop AEMs with good chemical stability. The chemical stability was evaluated by immersing membrane M3 or N3 into stirred 6 mol L^{-1} NaOH solution at 60 °C and measured the changes of ionic conductivity and IEC at intervals at 25 °C. Before the test, all the membrane samples should be washed by D.I. water numerous times until neutral. The results are showed Fig. 7.

It shows that the ionic conductivities and IEC are relatively stable within 168 h. The slight fluctuation of the conductivities for M3 and N3 at initial time may be due to more hydroxyl ion soaked inside the membrane. After that, the conductivities of M3 and N3 tend to be stable around 1.97×10^{-2} S cm^{-1} and 1.45×10^{-2} S cm^{-1}, which may be benefit from the pendent quaternized pyrrolidonium functional groups and the cross-linked structure. The results also show that IEC of M3 and N3 are relatively stable around 1.550 mmol g^{-1} and 0.980 mmol g^{-1}. Only slight changes can be found compared with the conductivities and IEC of the contrast samples, which were measured in D.I water after treated with 1 mol L^{-1} NaOH solution at 25 °C using membrane M3 and N3. The results indicate that the membranes based on pyrrolidonium cation groups have good alkali resistance.

3.8. Dimensional stability and tensile strength

Dimensional stability and mechanical property of the wet and dry cross-linked membrane were tested and the results were listed in Table 7. The experiment results exhibit that the size of membranes increases to some extent after fully swelling in deionized water. Swelling degree of these two membranes were 5.57% and 4.71%, respectively. Relatively low water swelling degree of the membrane is attributed to the cross-linking treatment and would be helpful to the membrane electrode assembly (MEA) preparation.

The tensile strengths of the wet and dry membranes were about 18 MPa and 14 MPa, respectively. The results show that the membranes with the cross-linked structure possess sufficient mechanical strength for fuel cell applications.

3.9. Fabrication of MEA and fuel cell test

The previous experiment results show that both OH^- form membrane M3 and N3 have good chemical and physical properties and can be applied to fuel cell. Therefore, the membrane M3 and N3 were used for an initial MEA fabrication. The MEAs with 4 cm^2

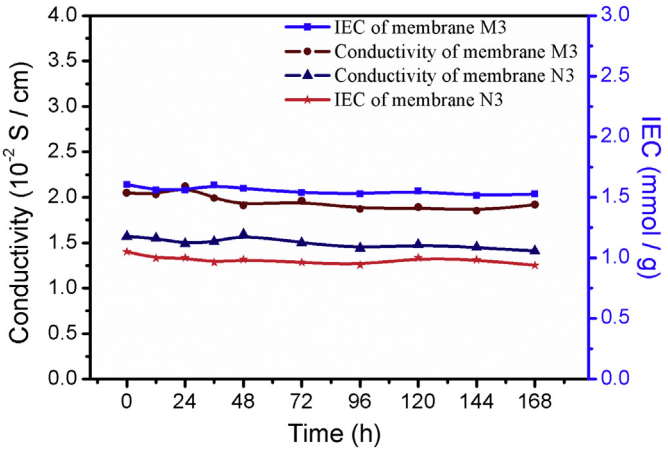

Fig. 7. The conductivities and IECs of membrane M3 and N3 after treatment with 6 mol L^{-1} NaOH at 60 °C.

Table 7
Swelling degree and tensile strength of the membranes.

Membranes	Condition	Length/cm	Swelling degree	Tensile/MPa
M3	Dry	7.00	5.57%	11.3
	Wet	7.39		17.9
N3	Dry	7.00	4.71%	14.3
	Wet	7.33		18.7

activated area and 1.2 mg cm^{-2} catalyst loading on the cathode and 0.8 mg cm^{-2} loading on the anode were prepared with membrane M3 (or N3) by hot pressing. The cells were activated with the current density of 100 mA cm^{-2} for 2 h at the beginning and then activated with the current density of 400 mA cm^{-2} for 2 h before the tests. In tests, the anode stream was hydrogen with flow rate of 600 mL min^{-1} and the cathode stream was air with flow rate of 800 mL min^{-1}, and the cell test temperature was 65 °C, relative humidity was 100%.

Fig. 8 shows the voltage–current density curves and the power density-current density curves of the cells under 100% humidity at ambient pressure. It is observed that the OCV of the H_2/air fuel cell with membrane M3 and N3 are 0.953 V and 0.933 V, respectively. The test results show that the peak power density of the H_2/air fuel cell with membrane M3 is 88.90 mW cm^{-2}, achieved at the current density of 175 mA cm^{-2}, higher than the maximum power density of the H_2/air fuel cell with membrane N3 (81.90 mW cm^{-2}, achieved at the current density of 200 mA cm^{-2}). It is corresponded to the higher ionic conductivity of membrane M3. It also shows that with the increasing of the current density, the voltage of the cell decreases gradually, which are mainly attributed to the electrode over potentials at high current densities [40]. In addition, the surface activity of the electrode and the interfacial property between the electrode and the membrane plays a significant role in the performance of the fuel cell [41]. In this work, we focus on the synthesis and characterization of the cross-linked membranes, studies on fabrication of MEA and fuel cell test remained preliminary. Future work will be devoted to the optimization of the electrode structure and testing conditions.

4. Conclusions

Two kinds of pyrrolidonium salts ionic liquids, NVMP and NVEP, have been successfully synthesized from NVP and halohydrocarbon (iodomethane or bromoethane). And their homopolymers, PNVMP and PNVEP, have been also successfully prepared. Two types of novel AAEMs have been prepared from PNVMP (or PNVEP) and PVA by a covalent cross-linking and solution casting method and applied to the H_2/air fuel cell test.

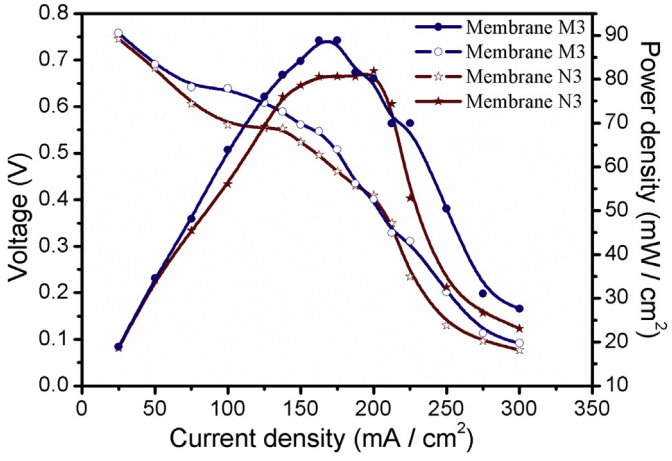

Fig. 8. Performance of the H_2/air fuel cells with membrane M3 and N3 at 65 °C.

The raw materials used in this study are relatively cheap, the preparation method is easy to manipulate and friendly to the environment. The effect of quaternarization time and different blends ratios of the casting solution have been studied. The resulting membrane M3 and N3 exhibit relatively high OH^- conductivities of 2.05×10^{-2} S cm^{-1} and 1.57×10^{-2} S cm^{-1}, fitting WU of 66.2% and 63.4%, and high IEC of 1.607 mmol g^{-1} and 1.052 mmol g^{-1} at 25 °C, respectively. The OH^- conductivities of the membrane M3 and N3 could be improved by raising the temperature, reaching to 4.98×10^{-2} S cm^{-1} and 4.14×10^{-2} S cm^{-1} at 85 °C, respectively. The resulting membrane M3 and N3 show excellent thermal stability with onset degradation temperature high above 235 °C, relatively good alkaline stability in 6 mol L^{-1} NaOH at 60 °C for 168 h and remarkable dimensional stability. The resulting membranes have been assembled into MEA and tested in the H_2/air single fuel cells. Test results show the OCV of 0.953 V and 0.933 V. The maximum power density of 88.90 mW cm^{-2} and 81.90 mW cm^{-2} at the current density of 175 mA cm^{-2} and 200 mA cm^{-2}, are obtained for fuel cells with M3 and N3, respectively. These results suggest that these membranes could be new prospects for use in alkaline fuel cells.

Acknowledgments

This work was financially supported by High-Tech Research and Development Program of China (No.2008AA05Z107) and National Nature Science Foundation of China Grant (Nos.20876129, 21376195 and 21321062).

References

[1] E.H. Yu, K. Scott, Development of direct methanol alkaline fuel cells using anion exchange membranes, J. Power Sources 137 (2004) 248–256.
[2] J. Bae, Control of microdomain orientation in block copolymer thin films by electric field for proton exchange membrane, Adv. Chem. Eng. Sci. 04 (2014) 95–102.
[3] K.A. Friedrich, P. Dimitrova, B. Vogt, U. Stimming, Transport properties of ionomer composite membranes for direct methanol fuel cells, J. Electro. Chem. 532 (2002) 75–83.
[4] J.W. Fergus, Materials challenges for solid-oxide fuel cells, JOM 59 (2007) 56–62.
[5] K.A. Mauritz, R.B. Moore, State of understanding of nafion, Chem. Rev. 104 (2004) 4535–4585.
[6] M. Ünlü, J. Zhou, I. Anestis-Richard, P.A. Kohl, Characterization of anion exchange ionomers in hybrid polymer electrolyte fuel cells, ChemSusChem 3 (2010) 1398–1402.
[7] T. Li, Y. Yang, A novel inorganic/organic composite membrane tailored by various organic silane coupling agents for use in direct methanol fuel cells, J. Power Sources 187 (2009) 332–340.
[8] L.A. Adams, S.D. Poynton, C. Tamain, R.C.T. Slade, J.R. Varcoe, A carbon dioxide tolerant aqueous-electrolyte-free anion-exchange membrane alkaline fuel cell, ChemSusChem 1 (2008) 79–81.
[9] J.R. Varcoe, R.C.T. Slade, E. Lam How Yee, S.D. Poynton, D.J. Driscoll, D.C. Apperley, Poly (ethylene-co-tetrafluoroethylene)-derived radiation-grafted anion-exchange membrane with properties specifically tailored for application in metal-cation-free alkaline polymer electrolyte fuel cells, Chem. Mater. 19 (2007) 2686–2693.
[10] J.R. Varcoe, R.C.T. Slad, Prospects for alkaline anion-exchange membranes in low temperature fuel cells, Fuel Cells 5 (2005) 187–200.
[11] M.A. Hickner, A.M. Herring, E.B. Coughlin, Anion exchange membranes: current status and moving forward, J. Phys. Chem. B 51 (2013) 1727–1735.
[12] J. Si, S. Lu, X. Xu, S. Peng, R. Xiu, Y. Xiang, A gemini quaternary ammonium poly (ether ether ketone) anion-exchange membrane for alkaline fuel cell: design, synthesis, and properties, ChemSusChem 7 (2014) 3389–3395.
[13] J. Wang, G. He, X. Wu, X. Yan, Y. Zhang, Y. Wang, Cross-linked poly (ether ether ketone) hydroxide exchange membranes with improved conductivity, J. Membr. Sci. 459 (2014) 86–95.
[14] J.S. Park, S.H. Park, S.D. Yim, Y.G. Yoon, W.Y. Lee, Performance of solid alkaline fuel cells employing anion-exchange membranes, J. Power Sources 178 (2008) 620–626.
[15] J. Fang, P.K. Shen, Quaternized poly (phthalazinon ether sulfone ketone)

membrane for anion exchange membrane fuel cells, J. Membr. Sci. 285 (2006) 317–322.
[16] J. Ran, L. Wu, Q. Ge, Y. Chen, T.W. Xu, High performance anion exchange membranes obtained through graft architecture and rational cross-linking, J. Membr. Sci. 470 (2014) 229–236.
[17] Hankun Xu, Jun Fang, Mingli Guo, Xiaohuan Lu, Xiaolan Wei, Song Tu, Novel anion exchange membrane based on copolymer of methyl methacrylate, vinylbenzyl chloride and ethyl acrylate for alkaline fuel cells, J. Membr. Sci. 354 (2010) 206–211.
[18] J. Ran, L. Wu, J.R. Varcoe, A.L. Ong, S.D. Poynton, Development of imidazolium-type alkaline anion exchange membranes for fuel cell application, J. Membr. Sci. 415–416 (2012) 242–249.
[19] F.L. Gu, H.L. Dong, Y.Y. Li, Z. Sun, F. Yan, Base stable pyrrolidinium cations for alkaline anion exchange membrane applications, Micromolecules 47 (2014) 6740–6747.
[20] B. Bauer, H. Strathmann, F. Effenberger, Anion-exchange membranes with improved alkaline stability, Desalination 79 (1990) 125–144.
[21] W. Li, J. Fang, M. Lv, C.X. Chen, X.J. Chi, Y.X. Yang, Novel anion exchange membranes based on polymerizable imidazolium salt for alkaline fuel cell applications, J. Mater. Chem. 21 (2011) 11340–11346.
[22] M. Guo, J. Fang, H. Xu, W. Li, X. Lu, C. Lan, K. Li, Synthesis and characterization of novel anion exchange membranes based on imidazolium-type ionic liquid for alkaline fuel cells, J. Membr. Sci. 362 (2010) 97–104.
[23] J. Fang, M. Lyu, X. Wang, Y.B. Wu, J.B. Zhao, Synthesis and performance of novel anion exchange membranes based on imidazolium ionic liquids for alkaline fuel cell applications, J. Power Sources 284 (2015) 517–523.
[24] L. Lebrun, N. Follain, M. Metayer, Elaboration of a new anion-exchange membrane with semi-interpenetrating polymer networks and characterization, Electrochim. Acta 50 (2004) 985–993.
[25] L. Lebrun, E. Da Silva, M. Metayer, Elaboration of ion-exchange membranes with semi- interpenetrating polymer networks containing poly (vinyl alcohol) as polymer matrix, J. Appl. Polym. Sci. 84 (2002) 1572–1580.
[26] B. Ding, H.Y. Kim, S.C. Lee, D.R. Lee, K.J. Choi, Preparation and characterization of nanoscaled poly(vinyl alcohol) fibers via electrospinning, Fibers Polym. 3 (2002) 73–79.
[27] J.I. Lim, M.J. Kang, W.K. Lee, Lotus-leaf-like structured chitosan–polyvinyl pyrrolidone films as an anti-adhesion barrier, Appl. Sur. Sci. 320 (2014) 614–619.
[28] D. Demberelnyamba, B.K. Shin, H. Lee, Ionic liquids based on N-vinyl-γ-butyrolactam: potential liquid electrolytes and green solvents, Chem. Commun. (2002) 1538–1539.
[29] M. Higa, M. Kobayashi, Y. Kakihana, A. Jikihara, N. Fujiwara, Charge mosaic membranes with semi-interpenetrating network structures prepared from a polymer blend of poly(vinyl alcohol) and polyelectrolytes, J. Membr. Sci. 428 (2013) 267–274.
[30] W. Garcia-Vasquez, L. Dammak, C. Larchet, V. Nikonenko, N. Pismenskaya, D. Grande, Evolution of anion-exchange membrane properties in a full scale electrodialysis stack, J. Membr. Sci. 446 (2013) 255–265.
[31] A.K. Shailesh, M. Kolhe, Preparation of strong base anion exchange membrane using 60Co gamma radiation, Radiat. J. Chem. Phys. 74 (2005) 384–390.
[32] Y. Xiong, Q.L. Liu, Q.H. Zeng, Quaternized cardo polyetherketone anion exchange membrane for direct methanol alkaline fuel cells, J. Power Sources 193 (2009) 541–546.
[33] J. Zhang, J. Qiao, G. Jiang, L. Liu, Y. Liu, Cross-linked poly(vinyl alcohol)/poly (diallyl dimethyl ammonium chloride) as anion-exchange membrane for fuel cell applications, J. Power Sources 240 (2013) 359–367.
[34] Y. Wu, C. Wu, J.R. Varcoe, S.D. Poynton, T.W. Xu, Novel silica/poly(2,6-dimethyl-1,4- phenylene oxide) hybrid anion-exchange membranes for alkaline fuel cells: Effect of silica content and the single cell performance, J. Power Sources 195 (2010) 3069–3076.
[35] Y.J. Wang, J. Qiao, R. Baker, J. Zhang, Alkaline polymer electrolyte membranes for fuel cell applications, Chem. Soc. Rev. 42 (2013) 5768–5787.
[36] J. Pan, C. Chen, L. Zhuang, J.T. Lu, Designing advanced alkaline polymer electrolytes for fuel cell applications, Acc. Chem. Res. 45 (2012) 473–481.
[37] M.S.P. Shaffer, A.H.F. Windle, Fabrication and characterization of carbon nanotube/poly(vinyl alcohol) composites, Adv. Mater. 11 (1999) 937–941.
[38] M.I. Loria-Bastarrachea, W. Herrera-Kao, J.V. Cauich-Rodriguez, et al., A TG/FTIR study on the thermal degradation of poly(vinyl pyrrolidone), J. Therm. Anal. Calorim. 104 (2011) 737–742.
[39] G. Wang, Y. Weng, D. Chu, R. Chen, D. Xie, Developing a polysulfone-based alkaline anion exchange membrane for improved ionic conductivity, J. Membr. Sci. 332 (2009) 63–68.
[40] J.H. Kim, H.K. Kim, K.T. Hwang, J.Y. Lee, Performance of air-breathing direct methanol fuel cell with anion-exchange membrane, Int. J. Hydrogen Energy 35 (2010) 768–773.
[41] E. Agel, J. Bouet, J.F. Fauvarque, Characterization and use of anionic membranes for alkaline fuel cells, J. Power Sources 101 (2001) 267–274.